Autophagy Induction in *C12orf65* Mutation-related Autosomal Recessive Hereditary Spastic Paraplegia

Li Wu
Department of Neurology, Shanghai Ninth People's Hospital, School of Medicine, Shanghai Jiao Tong University

Yang Xu
Laboratory of Molecular Neurobiology, School of Life Science and Biotechnology, Shanghai Jiao Tong University

Qin Wang
Department of Neurology, Zhongshan Hospital Fudan University

Zhi-Ping Xie
Sheng Yushou Center of Cell Biology and Immunology, Department of Genetics and Developmental Biology, School of Life Science and Biotechnology, Shanghai Jiao Tong University

You-Rong Dong
Department of Neurology, Shanghai Ninth People's Hospital, School of Medicine, Shanghai Jiao Tong University

Jian-Ren Liu
Department of Neurology, Shanghai Ninth People's Hospital, School of Medicine, Shanghai Jiao Tong University

Ilya A. Vinnikov
Laboratory of Molecular Neurobiology, School of Life Science and Biotechnology, Shanghai Jiao Tong University

Qing-Xuan Lai
Laboratory of Molecular Neurobiology, School of Life Sciences and Biotechnology, Shanghai Jiao Tong University

Wei Chen (david_chen8106@hotmai.com)
Department of Neurology, Shanghai Ninth People's Hospital, School of Medicine, Shanghai Jiao Tong University, Shanghai, 200011, China

---

Research article

Keywords: Hereditary spastic paraplegia type 55, C12orf65, LC3B, Autophagy

Posted Date: January 4th, 2021

DOI: https://doi.org/10.21203/rs.3.rs-136140/v1

Abstract

Background: Spastic paraplegia type 55 (SPG55) is an autosomal recessive complicated hereditary spastic paraplegia. Here we report an SPG55 case with typical neurological phenotypes including optic atrophy, lower extremity spasticity and peripheral neuropathy.

Methods: The present study involved one patient in a Chinese family. Neurological examination including the ophthalmology related examinations as well as nerve conduction velocity and a sural nerve biopsy were performed for the patient. We performed a genetic analysis of genes associated with peripheral neuropathy and spastic paraplegia using a multigene next-generation sequencing(NGS) panel and sanger sequencing. Furthermore, we cultured patient's primary skin fibroblasts, then we examined the cytoplasmic LC3B immunofluorescence in the patient's primary fibroblast and after two drugs (butylphthalide sodium chloride and idebenone) were used to the target the mitochondria function of the fibroblast.

Results: Here we reported an SPG55 case with typical neurological phenotypes including optic atrophy, lower extremity spasticity and peripheral neuropathy. We identified a homozygous *C12orf65* nonsense mutation (c.394C>T, p. R132*) in the affected patient. The mutation was associated with active autophagosome formation with increased LC3B puncta in the patient's fibroblasts compared with an age-matched healthy individual, while the latter phenotype was normalized by Dl-3-N-butylphthalide treatment.

Conclusions: This is the first pilot study to characterize the SPG55 mutation in the Chinese population; it will contribute to further research revealing the role of *C12orf65* mutations in regulation of mitochondria function and autophagy.

Background

Hereditary spastic paraplegia is a clinically and genetically heterogeneous group of inherited neurodegenerative disorders in which the main neurological symptoms comprise progressive spasticity and weakness of the lower limbs [1, 2]. So far, 79 genes have been linked to spastic paraplegia (SPG1-SPG79, in the order of discovery) with X-linked, autosomal dominant or recessive inheritance, with or without maternal imprinting [3]. Spastic paraplegia type 55 (SPG55) is an autosomal recessive pathology caused by homozygous mutation in the *Chromosome 12 open reading frame 65* (*C12orf65*) gene mapped to chromosome 12q24.31[4]. SPG55 varies in disease phenotypes including early onset slowly progressive spastic paraplegia, progressive visual loss with optic atrophy, distal axonal motor and sensory neuropathy, delayed psychomotor development with mental retardation, pes equinovarus, and arthrogryposis. Neuroimaging studies demonstrated hypoplastic corpus callosum in some patients [2, 5].

C12orf65 is a nuclear gene encoding a mitochondrial matrix protein which is critical for the release of newly synthesized proteins from mitochondrial ribosomes [6]. Shimazak *et al.* identified a homozygous truncating mutation in *C12orf65* causing reduced synthesis of most mitochondrial proteins and reduced

activities of some respiratory complex enzymes [2]. These findings indicated that defects in mitochondrial translation may be a mechanism underlying degeneration of the corticospinal tracts and spastic paraplegia.

Importantly, reduced ATP levels due to decreased activity of ATP synthase may cause autophagy through the Amp-activated protein kinase (AMPK) pathway [7]. AMPK is a major metabolic energy sensor that regulates energy homeostasis by controlling several homeostatic mechanisms, including autophagy [8, 9]. AMPK serves as a positive regulator of autophagy mainly via inhibiting the mammalian target of rapamycin (mTOR) complex and phosphorylating unc-51-like kinase 1 (ULK1, the ortholog of Atg1 in mammals) [10, 11]. Furthermore, the defective mitochondrial function in patients with hereditary spastic paraplegia might cause PINK1 (PTEN-induced putative kinase 1) and the E3 ligase Parkin1-dependent activation of mitophagy, a variant of autophagy associated with mitochondria recycling [12–14]. Indeed, Chang *et al.* identified a depletion of free lysosomes and an accumulation of autolysosomes due to an impaired lysosome formation upon the loss of function of SPG11/15 [15].

The precise pathogenesis mechanism of SPG55 is still unclear. In the current work, we present a patient with a unique combination of early onset optic atrophy, progressive distal lower extremity spasticity and sensorimotor peripheral neuropathy. We demonstrate that a nonsense mutation in *C12orf65* is associated with an increased number of microtubule-associated proteins 1A/1B LC3B-positive puncta detected in fibroblasts from SPG55 patient.

Methods

Human subjects

The proband was a patient observed in Department of Neurology, Shanghai Ninth People's Hospital, School of Medicine, Shanghai Jiao Tong University, Shanghai, China. Peripheral venous blood from the patient and his family members was collected for genetic analyses. Primary fibroblasts were isolated from skin biopsy samples of the patient and an age-matched healthy volunteer. Informed consent was obtained from all subjects involved according to the Helsinki Declaration. The study was approved by the Ethics Committee of Shanghai Ninth People's Hospital, School of Medicine, Shanghai Jiao Tong University.

Next-generation Sequencing Analysis And Sanger Sequencing

Genomic DNA was extracted using QIAamp DNA extraction kit (QIAGEN), and the concentration was measured. DNA was then fragmented by DNase and purified by magnetic bead method, followed by PCR amplification and ligation of the adapter sequences. Further, it was captured and purified twice by a custom Panel probe (Illumina Inc, USA), and then amplified by PCR. The final library obtained after

purification was used to sequence exon regions of Panel-related genes on a NextSeq500 sequencer (Illumina Inc, USA). All data were compared to the reference sequence (UCSC hg19) using the BWA algorithm with the instrument's default settings [16] and data reporting methods for annotation [17]. By implementing clinical data and the prediction results of bioinformatics software including PolyPhen2, LRT, Mutation Taster, the functional, mutation and genetic patterns of each gene were screened to obtain the list of candidate mutations. PCR primers were designed for the sites of candidate mutations in the patient's parents for amplification and Sanger sequencing verification.

Primary Fibroblast Culture

Briefly, after local sterilization and anesthesia, full-thickness skin biopsies (~ 5 mm^3) were taken from the patient and a 25-year-old healthy volunteer. The isolates were placed into 50-ml conical tubes filled with biopsy culture medium containing 400 ml minimum essential medium, 100 ml fetal bovine serum, 5 ml penicillin/streptomycin solution (10,000 U/ml penicillin G and 10,000 µg/ml streptomycin) and stored in culture medium for 12 hours at 4 °C before dissection for primary culture. After removing the biopsy culture medium, the biopsy samples were washed three times with 10 ml DPBS without calcium and magnesium. Further, they were placed to a sterile 6-cm tissue culture dish containing ~ 7 ml primary culture medium containing 400 ml minimum essential medium, 100 ml fetal bovine serum, 5 ml penicillin/streptomycin/Fungizone solution (10,000 U/ml penicillin G, 10,000 µg/ml streptomycin, 25 µg/ml amphotericin B) and anti-mycoplasma reagent. The biopsies were first cut into small pieces, then refined to pieces with the size of a pinhead. Further, we placed each 10 pinhead-sized explants into one 25-cm^2 tissue culture–treated flask (Nunc™ EasYFlask™ 156340), waited for 20 minutes for the explants to adhere and added 12 ml primary culture medium. The flasks were placed into a dedicated 37 °C, 5% CO_2 incubator for 5 days, followed by replacement of the medium by fresh primary culture medium. The fibroblast cultures were further maintained, checked daily for growth, confluence and contamination, with medium replacements every 3–5 days according to Villegas et al [18]. When the confluence was ~ 95%, the passage 2 fibroblasts from patient and healthy volunteer were seeded into two 96-well plates with the densities 3–9 × 10^3 cells/ml. Drug treatment was started when the confluence reached 60%~70%. Two drugs were used to target the mitochondria function of the fibroblasts. Butylphthalide sodium chloride (further referred to as butylphthalide, EnBiPu, CSPC NMP pharmaceutical company, H20100041) was diluted from the 25 mg/100 ml 0.9% sodium chloride stock solution in DMEM and used in final concentrations 10 µM and 26.28 µM. 70 mM idebenone stock solution was made by dissolving 30 mg tablets (Qilu Pharmaceutical Co., H10970137) in 0.2% DMSO, followed by dilution in DMEM to get a 5 µM final concentration. After addition of the drugs, the fibroblasts were incubated 48 hours in a 37 °C, 5% CO_2 humidified incubator followed by immunofluorescent analysis. The cells were incubated for one hour with 1:20000 MitoTracker Orange (Molecular probes M7510) in a 37 °C, 5% CO_2 humidified incubator). Further, we incubated with 1:20000 Hoechst 33342 (Invitrogen, #H3570) in 1 × PBS for 5 minutes at room temperature. Then the cells were fixed in 4% PFA (Aladdin, C104188) for 20 minutes, washed twice with 1 × PBS, permeabilized with 0.2% Triton X-100 for 15 minutes, blocked by

0.2% Triton X-100, 5% normal goat serum (Biotopped, SU3757) in PBS for 1 hour at room temperature. 1:1000 anti-LC3B primary antibody (Thermo Fisher, PA5-30598) diluted in 1 × PBS with 0.2% Triton X-100, 5% serum, was incubated overnight at 4 °C followed by washing and incubation for 1 hour at room temperature in 2 µg/ml of anti-rabbit IgG (H + L) highly cross absorbed secondary antibody conjugate with Alexa Fluor Plus 647 (Thermo A-21245), diluted in 1 × PBS with 0.2% Triton X-100. LC3B and MitoTracker signal was visualized under an Olympus IX73 microscope after immunocytochemistry staining. COOLLED PE300 were used as the illumination sources. Fluorescence emission was collected by 60 × objective, passed through EM 680/40 and EM 617/73 emission filters for LC3B and MitoTracker, respectively. All the images were acquired and processed by Micro-Manager software. The same conditions were applied to all samples. Fluorescence intensity was quantified by calculating the average cytoplasmic LC3B signal normalized to the number of cells by using MCID and Prism (GraphPad) software.

Statistical analysis

For the in vitro experiment's analyses, we used ordinary two-way ANOVA followed by Holm-Sidak's multiple comparisons test vs. each healthy individual's fibroblasts in every treatment group and ordinary one-way ANOVA followed by Holm-Sidak's multiple comparisons test at all treated patient groups vs. the untreated patient group. The levels of significance were set at $*P < 0.05$ and $**P < 0.001$. Values were presented as mean ± standard error of mean (SEM).

Results

Clinical details

The proband was a 30-year-old man, who visited our hospital because of decreased visual acuity and slowly progressive weakness of the lower extremities. His delivery was normal, with normal motor and mental development in infancy. Retrospectively, the patient's progressive loss of visual acuity at the age of nine was the first reported symptom. One year later, he developed muscle atrophy and fatigue of both lower limbs, foot drop leading to a steppage gait and slowly developing weakness of the lower extremities. No history of learning difficulties or seizures had been detected.

Neurological examination on admission at the age of 30 revealed loss of visual acuity with bilateral optic atrophy (Fig. 1A): the naked eye vision was scored as 0.2/1.0 and 0.05/1.0 (left and right eyes, respectively) without any macular morphology abnormalities on both sides, as revealed by *in vivo* optical coherence tomography (Fig. 1B).

The muscle strength was normal in the upper limbs, however the lower limbs were scored as 4/5 in foot flexion (Medical Research Council Scale, Grade 0–5) [19]and 2/5 in foot dorsiflexion. Marked distal symmetrical wasting affected the bilateral lower limbs (Fig. 1. **C**). The feet appeared to have a pes cavus deformity, with a flexion contracture of the toes. In addition to the brisk reflexes of all extremities, there

were no other pyramidal signs. Minor asymmetric postural tremor was observed in this patient without cerebellar ataxia. Sensitivity to pinprick, touch, temperature, positioning and vibration was normal in all the limbs.

Nerve conduction velocity studies revealed a demyelinating and axonal sensory and motor peripheral neuropathy. The compound muscle action potential of bilateral tibialis and common peroneal nerves was not elicited. Decreases in the sensory conduction velocity (SCV) and in the sensory nerve action potential (SNAP) amplitude were observed in ulnar and peroneal nerves on both sides (left ulnar sensory: SCV 38.5 m/s with SNAP amplitude 17 mV; left peroneal sensory: 35.3 m/s with 6.2 mV; right peroneal sensory: 27.4 m/s with 0.1 mV). Needle electromyography showed positive shape waves and high motor unit potential in most muscles of lower and upper extremities, indicating both chronic and active loss of innervations in these muscles.

A sural nerve biopsy demonstrated a predominantly chronic demyelinating neuropathy (Fig. 1D-G). Electron microscopy imaging revealed a slight loss of myelinated fibers and multiple fibers with extremely thin myelin sheaths, indicating a defective myelination. Schwann cell degeneration was apparent in the patient as demonstrated by increased perinuclear π particles in Schwann cells, and shingled Schwann cell processes around the unmyelinated fibers.

Identification of a C12orf65 mutation

The *C12orf65* gene (c.394C > T) [NM_152269.4] homozygous point mutation in the spastic paraplegia patient was identified using next-generation sequencing (Fig. 2A). The variant causes an arginine 132 substitution by a stop codon (p.R132*) in the release factor-1 (RF-1) domain (Fig. 2B). Next, we sequenced this locus in every volunteer in this pedigree revealing an asymptomatic carriers of the heterozygous c.394C > T mutation indicated in Fig. 2C as IV2, IV6, IV7, IV10 and V4.

Increased LC3B signal in primary fibroblasts from the SPG55 patient

Consistent with other studies [2, 20], we discovered no morphological changes in mitochondria such as increased fragmentation, fission or fusion in the SPG55 patient primary fibroblasts (Fig. 3A). In order to study whether the defective mitochondrial translation in SPG55 could trigger reactive autophagy, we examined the abundance of cytoplasmic puncta positive for LC3B, a common marker for autophagic structures. Indeed, we detected a significant increase in cytoplasmic LC3B immunofluorescence (Fig. 3B) in primary fibroblast cultures from the SPG55 patient compared to an age-matched healthy individual. Butylphthalide and idebenone are promising candidate drugs for mitochondrial protection. Butylphthalide has been reported to restore mitochondrial membrane potential and prevent reactive oxygen species (ROS) generation [21]. Idebenone is a potent antioxidant and inhibitor of lipid peroxidation, interacting with the mitochondrial electron transport chain and facilitating mitochondrial electron flux in bypassing complex [22]. As such, we sought to explore whether these drugs could normalize the autophagy-related phenotype detected in SPG55 primary fibroblasts. Indeed, we observed a tendency towards attenuation of the patient fibroblasts' LC3B signal upon idebenone or butylphthalide treatment (with the latter reaching a

statistical significance at the concentration of 26 μM), supporting a key role of mitochondrial defects in the observed autophagy induction (Fig. 3).

Discussion

In previous studies, all clinically relevant *C12orf65* mutations were truncating, including nonsense mutations (p.L94*, p.V116*, p.R132* and p.R139*) and frameshift mutations (p.T2Rfs*54, p.P34Ifs*25, p.V83Gfs*2, p.G72Afs*13 and p.K138Rfs*17) (Fig. 2A, B) with the mutation sites located in the release factor-1 (RF-1) domain, with the exception of p.K138Rfs*17 [2, 26, 23, 24]. Disease severity has been previously reported to depend on the residual length of the truncated *C12orf65* protein. Indeed, patients with truncating mutations close to the N-terminal demonstrate severe phenotypes, including neonatal death, optical atrophy and severe cognitive dysfunction in addition to the main symptoms. In contrast, patients with truncations close to the C-terminus showed only mild intellectual disability associated with the main symptoms [25]. In the current study, homozygous p.R132* mutation close to the C-terminus resulted in an optic atrophy with reduced visual acuity, lower limb spasticity with peripheral neuropathy. Recently, a Japanese group has reported the same mutation site resulting in almost the same clinical manifestations as in our patient (Shimazaki, Takiyama et al. 2012). They detected that the c.394C > T mutation was associated with optic atrophy and peripheral neuropathy in addition to the main symptoms [2]. Thus, it can be inferred that the above three signs may be characteristic for this nonsense mutation.

Consistent with the critical role of *C12orf65* in releasing newly synthesized mitochondrial proteins, SPG55 cases were found to be associated with decreases in respiration, in ATP synthase activity and in mitochondrial membrane potential [26]. As mentined above, Shimazaki *et al.* described an SPG55 patient with the identical c.394C > T mutation [2]. In that study, patient-derived fibroblasts were found to have a decrease in expression of most mitochondrial proteins and reduced activities of respiratory complex enzymes including complexes I, III and IV indicating a profound mitochondrial defect associated with this mutation [2]. Balanced mitochondrial biogenesis and mitochondrial quality control helps remain mitochondria function in neurons [27]. In our study, we sought to analyze the morphology of mitochondria and autophagosomes in patient-derived primary fibroblasts. There, we detected a prominent enrichment of cytoplasmic LC3B-positive puncta compared to an age-matched healthy individual (Fig. 3A). These data suggest a reactive over-activation of autophagosome formation in response to the mitochondria impairment, as previously described [28]. The mechanism of selective tagging of damaged mitochondria by such control mechanism has been largely attributed to the coordinated action of PTEN-induced putative kinase (PINK1) and Parkin [29]. As such, defective mitochondria normally trigger PINK1/Parkin-dependent activation of mitophagy [30]. Furthermore, mutations in autophagy-related genes have been reported in spastic paraplegia patients [31, 32]. Interestingly, tectonin beta-propeller repeat-containing protein 2 (TECPR2), the causative gene in SPG 49, has been previously found to interact with autophagy-related 8 orthologues [31, 33]. Moreover, since the activity of ATP synthase has been reported to be reduced in patients with *C12orf65* inactivation (see above) [26], reduced ATP levels could trigger the AMPK-mediated mTOR pathway inhibition and ULK1 phosphorylation and thus induction of autophagy [34, 35]. Indeed, our study showed that application of

butylphthalide can attenuate the LC3B phenotype in the SPG55 patient-derived fibroblasts. Therefore, this autophagy induction could represent a compensatory reaction on the accumulation of defective mitochondria. Butylphthalide is a synthetic compound that had been approved by the State Food and Drug Administration of China for the treatment of ischemic stroke in 2002. Interestingly, previous *in vivo* and *in vitro* studies have reported that this drug can attenuate neuronal autophagy [36, 37]. Although the positive effects of butylphthalide on brain vascular and neurodegenerative diseases has been verified in many experiments, its effects on SPG-related pathologies remain to be addressed in detail.

Conclusions

In summary, in the present study we described a typical case of complicated hereditary spastic paraplegia manifesting an early onset of optic atrophy, progressive lower extremity spasticity, and distal peripheral neuropathy, resulting from a nonsense c.394C > T, p.R132* mutation in *C12orf65*. Active autophagosome formation with increased LC3B puncta was found in the patient's fibroblasts, and its level was normalized when treated by Dl-3-N-butylphthalide. Thus our study deepens the clinical and molecular characterization of SPG55 and suggests a potential therapeutic approach to treat spastic paraplegia.

Abbreviations

SPG55
Spastic paraplegia type 55
NGS
next-generation sequencing
AMPK
Amp-activated protein kinase
mTOR
mammalian target of rapamycin
ULK1
phosphorylating unc-51-like kinase
PINK1
PTEN-induced putative kinase 1
SEM
standard error of mean
SCV
sensory conduction velocity
SNAP
sensory nerve action potential
ROS
reactive oxygen species

RF-1
release factor-1
TECPR2
tectonin beta-propeller repeat-containing protein 2

Declarations

Ethics approval and consent to participate

The study was approved by the Ethics Committee of Shanghai Ninth People's Hospital, School of Medicine, Shanghai Jiao Tong University. Written informed consent was obtained from the parents to take part in this study and for possible publication. A copy of the written consent is available for review by the Editor of this journal.

Consent for publication

Written informed consents for publication of clinical details and clinical images were obtained from participants

Availability of data and material

The dataset used and analyzed during the current study are available from the corresponding author on reasonable request.

Competing interests

The authors report no conflicts of interest.

Funding

This study was supported in part by the National Natural Science Fund of China 81401039, Shanghai medical guidance program 17411964000, Shanghai Pujiang Program 18PJD023, Startup Fund for Youngman Research at SJTU AF0800059, Shanghai young science and technology talents Sailing Program 18YF1412600, as well as the Interdisciplinary Program of Shanghai Jiao Tong University YG2017QN13. The funder had no role in the design of the study and collection, analysis, and interpretation of data and in writing the manuscript.

Authors' contributions

WC: ideated the study; LW and WC: collected the subjects; WC, QW and LW: performed the clinical examinations; ZPX, IAV and QXL: conceptualized the in vitro experiments; YX and QXL: performed the in vitro experiments and analysis; LW, XY, IAV, QXL and WC: wrote the paper; YRD and JRL: reconfirmed clinical diagnosis and clinical features

All authors read and approved the manuscript.

Acknowledgements

The authors express their sincere gratitude to the participants for their help and willingness to participate in this study.

We thank the patients and all the participants for cooperating our investigation and acknowledge the professionalism and compassion demonstrated by the healthcare workers involved in patients' care. The authors gratefully acknowledge the financial supports by the National Natural Science Fund of China 81401039, Shanghai medical guidance program 17411964000, Shanghai Pujiang Program 18PJD023, Startup Fund for Youngman Research at SJTU AF0800059, Shanghai young science and technology talents Sailing Program 18YF1412600, as well as the Interdisciplinary Program of Shanghai Jiao Tong University YG2017QN13.We also thank the patients for cooperating with our investigation and acknowledge the professionalism and compassion demonstrated by all the healthcare workers involved in patients' care.

References

1. Harding, A. E. (1983). "CLASSIFICATION OF THE HEREDITARY ATAXIAS AND PARAPLEGIAS." The Lancet 321(8334): 1151-1155.
2. Shimazaki, H., Y. Takiyama, H. Ishiura, C. Sakai, Y. Matsushima, H. Hatakeyama, J. Honda, K. Sakoe, T. Naoi, M. Namekawa, Y. Fukuda, Y. Takahashi, J. Goto, S. Tsuji, Y.-i. Goto and I. Nakano (2012). "A homozygous mutation of C12orf65 causes spastic paraplegia with optic atrophy and neuropathy (SPG55)." Journal of Medical Genetics 49(12): 777.
3. de Souza, P. V. S., W. B. V. de Rezende Pinto, G. N. de Rezende Batistella, T. Bortholin and A. S. B. Oliveira (2017). "Hereditary spastic paraplegia: clinical and genetic hallmarks." The Cerebellum 16(2): 525-551.
4. Kumar, K. R., N. F. Blair and C. M. Sue (2015). "An update on the hereditary spastic paraplegias: new genes and new disease models." Movement disorders clinical practice 2(3): 213-223.
5. Fink, J. K. (2013). "Hereditary spastic paraplegia: clinico-pathologic features and emerging molecular mechanisms." Acta neuropathologica 126(3): 307-328.
6. Antonicka, H., E. Østergaard, F. Sasarman, W. Weraarpachai, F. Wibrand, A. M. B. Pedersen, R. J. Rodenburg, M. S. Van der Knaap, J. A. Smeitink and Z. M. Chrzanowska-Lightowlers (2010). "Mutations in C12orf65 in patients with encephalomyopathy and a mitochondrial translation defect." The American Journal of Human Genetics 87(1): 115-122.
7. Zhang, C.-S. and S.-C. Lin (2016). "AMPK promotes autophagy by facilitating mitochondrial fission." Cell metabolism 23(3): 399-401.
8. Hardie, D. G. (2007). "AMP-activated protein kinase as a drug target." Annu. Rev. Pharmacol. Toxicol. 47: 185-210.

9. Vingtdeux, V., P. Chandakkar, H. Zhao, C. d'Abramo, P. Davies and P. Marambaud (2011). "Novel synthetic small-molecule activators of AMPK as enhancers of autophagy and amyloid-β peptide degradation." The FASEB Journal 25(1): 219-231.
10. Kim, J., M. Kundu, B. Viollet and K.-L. Guan (2011). "AMPK and mTOR regulate autophagy through direct phosphorylation of Ulk1." Nature cell biology 13(2): 132-141.
11. Hoeffer, C. A., E. Sanchez, R. J. Hagerman, Y. Mu, D. V. Nguyen, H. Wong, A. M. Whelan, R. S. Zukin, E. Klann and F. Tassone (2012). "Altered mTOR signaling and enhanced CYFIP2 expression levels in subjects with fragile X syndrome." Genes, Brain and Behavior 11(3): 332-341.
12. Narendra, D. P., S. M. Jin, A. Tanaka, D.-F. Suen, C. A. Gautier, J. Shen, M. R. Cookson and R. J. Youle (2010). "PINK1 is selectively stabilized on impaired mitochondria to activate Parkin." PLoS biology 8(1).
13. Vincow, E. S., G. Merrihew, R. E. Thomas, N. J. Shulman, R. P. Beyer, M. J. MacCoss and L. J. Pallanck (2013). "The PINK1–Parkin pathway promotes both mitophagy and selective respiratory chain turnover in vivo." Proceedings of the National Academy of Sciences 110(16): 6400-6405.
14. Zhang, C., X. Yu, J. Gao, Q. Zhang, S. Sun, H. Zhu, X. Yang and H. Yan (2018). "PINK1/Parkin-mediated mitophagy was activated against 1, 4-Benzoquinone-induced apoptosis in HL-60 cells." Toxicology in Vitro 50: 217-224.
15. Chang, J., S. Lee and C. Blackstone (2014). "Spastic paraplegia proteins spastizin and spatacsin mediate autophagic lysosome reformation." The Journal of clinical investigation 124(12): 5249-5262.
16. Li, H. and R. Durbin (2010). "Fast and accurate long-read alignment with Burrows–Wheeler transform." Bioinformatics 26(5): 589-595.
17. Zhang, L., J. Zhang, J. Yang, D. Ying, Y. l. Lau and W. Yang (2013). "PriVar: a toolkit for prioritizing SNVs and indels from next-generation sequencing data." Bioinformatics 29(1): 124-125.
18. Villegas, J. and M. McPhaul (2005). "Establishment and culture of human skin fibroblasts." Current protocols in molecular biology Chapter28(1): Unit28.3.
19. James, M. A. (2007). "Use of the Medical Research Council muscle strength grading system in the upper extremity." Journal of Hand Surgery 32(2): 154-156.
20. Nishihara, H., M. Omoto, M. Takao, Y. Higuchi, M. Koga, M. Kawai, H. Kawano, E. Ikeda, H. Takashima and T. Kanda (2017). "Autopsy case of the C12orf65 mutation in a patient with signs of mitochondrial dysfunction." Neurology Genetics 3(4): e171.
21. Xiong, N., J. Huang, C. Chen, Y. Zhao, Z. Zhang, M. Jia, Z. Zhang, L. Hou, H. Yang, X. Cao, Z. Liang, Y. Zhang, S. Sun, Z. Lin and T. Wang (2012). "Dl-3-n-butylphthalide, a natural antioxidant, protects dopamine neurons in rotenone models for Parkinson's disease." Neurobiology of Aging 33(8): 1777-1791.
22. Haefeli, R. H., M. Erb, A. C. Gemperli, D. Robay, I. C. Fruh, C. Anklin, R. Dallmann and N. Gueven (2011). "NQO1-dependent redox cycling of idebenone: effects on cellular redox potential and energy levels." PloS one 6(3).

23. Buchert, R., S. Uebe, F. Radwan, H. Tawamie, S. Issa, H. Shimazaki, M. Henneke, A. B. Ekici, A. Reis and R. A. Jamra (2013). "Mutations in the mitochondrial gene C12ORF65 lead to syndromic autosomal recessive intellectual disability and show genotype phenotype correlation." European journal of medical genetics 56(11): 599-602.
24. Fang, X.-J., W. Zhang, H. Lyu, Z.-X. Wang, W.-W. Wang and Y. Yuan (2017). "Compound heterozygote mutation of C12orf65 causes distal motor neuropathy and optic atrophy." Chinese medical journal 130(2): 242-244.
25. Spiegel, R., H. Mandel, A. Saada, I. Lerer, A. Burger, A. Shaag, S. A. Shalev, H. Jabaly-Habib, D. Goldsher and J. M. Gomori (2014). "Delineation of C12orf65-related phenotypes: a genotype–phenotype relationship." European Journal of Human Genetics 22(8): 1019-1025.
26. Tucci, A., Y.-T. Liu, E. Preza, R. D. S. Pitceathly, A. Chalasani, V. Plagnol, J. M. Land, D. Trabzuni, M. Ryten, Z. Jaunmuktane, M. M. Reilly, S. Brandner, I. Hargreaves, J. Hardy, A. B. Singleton, A. Y. Abramov and H. Houlden (2014). Novel C12orf65 mutations in patients with axonal neuropathy and optic atrophy." Journal of Neurology, Neurosurgery & Psychiatry 85(5): 486.
27. Palomo, G. M., V. Granatiero, H. Kawamata, C. Konrad, M. Kim, A. J. Arreguin, D. Zhao, T. A. Milner and G. Manfredi (2018). "Parkin is a disease modifier in the mutant SOD1 mouse model of ALS." EMBO molecular medicine 10(10).
28. Kim, I., S. Rodriguez-Enriquez and J. J. Lemasters (2007). "Selective degradation of mitochondria by mitophagy." Archives of biochemistry and biophysics 462(2): 245-253.
29. Mouton-Liger, F., M. Jacoupy, J.-C. Corvol and O. Corti (2017). "PINK1/Parkin-dependent mitochondrial surveillance: from pleiotropy to Parkinson's disease." Frontiers in molecular neuroscience 10: 120.
30. Pickrell, A. M. and R. J. Youle (2015). "The roles of PINK1, parkin, and mitochondrial fidelity in Parkinson's disease." Neuron 85(2): 257-273.
31. Vantaggiato, C., C. Crimella, G. Airoldi, R. Polishchuk, S. Bonato, E. Brighina, M. Scarlato, O. Musumeci, A. Toscano and A. Martinuzzi (2013). "Defective autophagy in spastizin mutated patients with hereditary spastic paraparesis type 15." Brain 136(10): 3119-3139.
32. Jiang, P. and N. Mizushima (2014). "Autophagy and human diseases." Cell research 24(1): 69-79.
33. Oz-Levi, D., B. Ben-Zeev, E. K. Ruzzo, Y. Hitomi, A. Gelman, K. Pelak, Y. Anikster, H. Reznik-Wolf, I. Bar-Joseph and T. Olender (2012). "Mutation in TECPR2 reveals a role for autophagy in hereditary spastic paraparesis." The American Journal of Human Genetics 91(6): 1065-1072.
34. Behrends, C., M. E. Sowa, S. P. Gygi and J. W. Harper (2010). "Network organization of the human autophagy system." Nature 466(7302): 68-76.
35. Egan, D. F., D. B. Shackelford, M. M. Mihaylova, S. Gelino, R. A. Kohnz, W. Mair, D. S. Vasquez, A. Joshi, D. M. Gwinn and R. Taylor (2011). "Phosphorylation of ULK1 (hATG1) by AMP-activated protein kinase connects energy sensing to mitophagy." Science 331(6016): 456-461.
36. Peng, Y., Y. Hu, S. Xu, P. Li, J. Li, L. Lu, H. Yang, N. Feng, L. Wang and X. Wang (2012). "L-3-n-butylphthalide reduces tau phosphorylation and improves cognitive deficits in AβPP/PS1-Alzheimer's

transgenic mice." Journal of Alzheimer's Disease 29(2): 379-391.

37. Zhang, T., H. Wang, Q. Li, J. Huang and X. Sun (2014). "Modulating autophagy affects neuroamyloidogenesis in an in vitro ischemic stroke model." Neuroscience 263: 130-137.

Figures

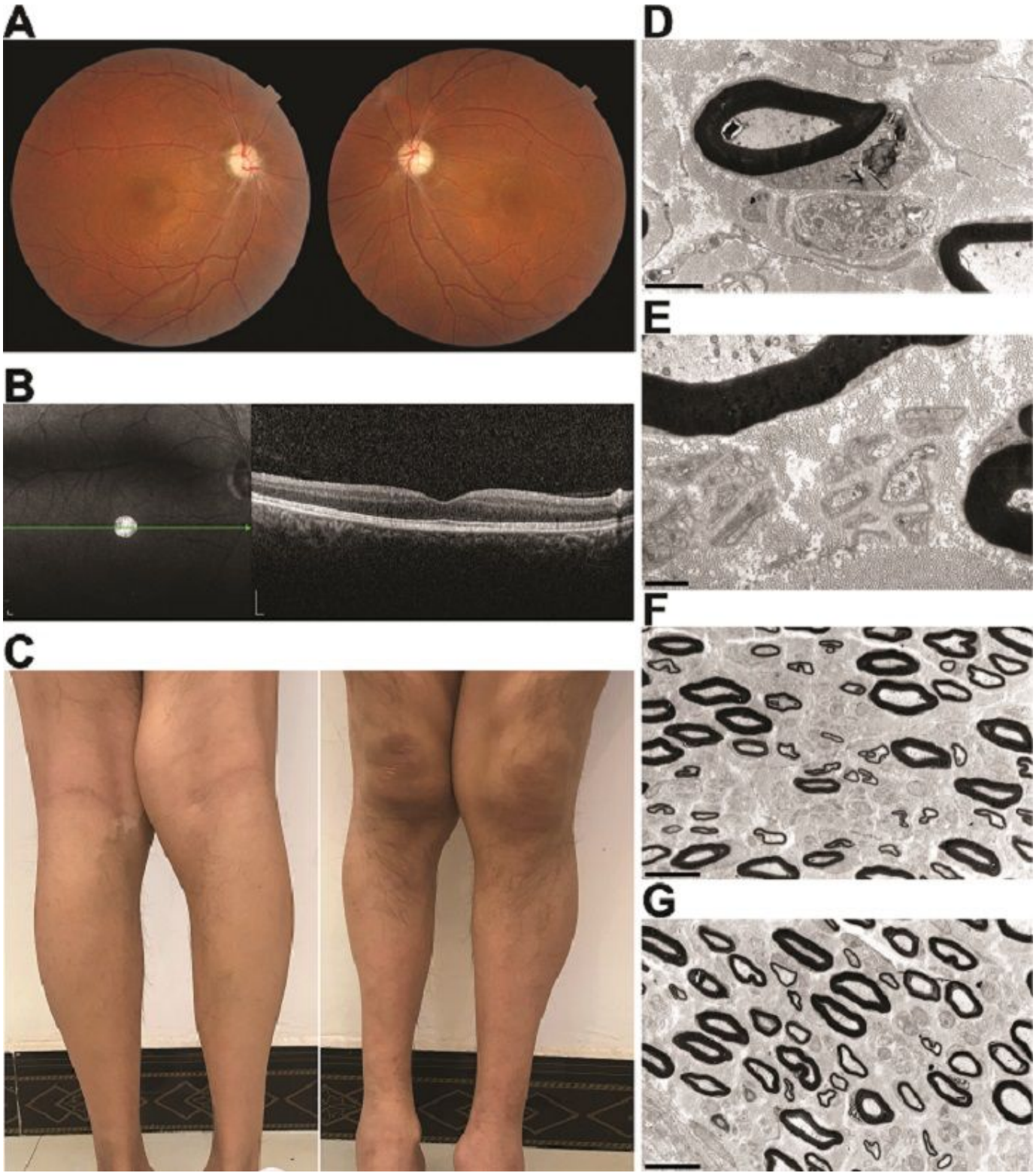

Figure 1

Clinical and morphological characterization of the spastic paraplegia type 55 case. A, Fundus photography of the left and right eyes from the patient revealed the pale optic nipples, indicating the optic atrophy. B, Optical coherence tomography of patient depicted a normal retina morphology. C, Muscle atrophy of the distal lower extremities. The right gastrocnemius atrophy is more pronounced. D-G, Ultrastructured electron microscopy images of a sural nerve biopsy samples reveal chronic defective myelination, Schwann cells degeneration, multiple fibers with extremely thin myelin sheaths, perinuclear π particles in Schwann cells, shingled Schwann cell processes around unmyelinated fibers. Scale bars: D, 2.5μm, E, 1 μm; F, 10 μm and G, 10μm.

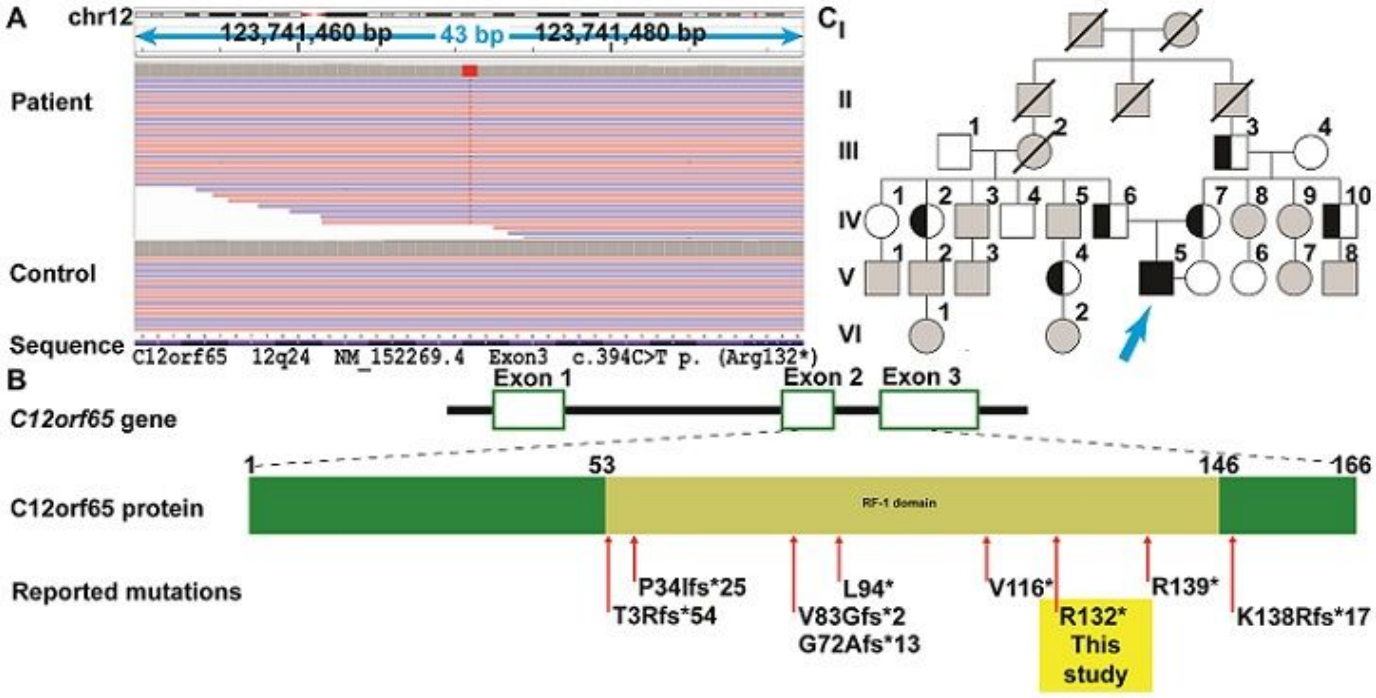

Figure 2

Genetic characterization of SPG55. A, Sequencing data showing the homozygous mutation c.394C>T in the patient. Upper panel: next-generation sequencing data for the c. 394C>T mutation in C12orf65. Lower panel: next-generation sequencing data for the normal C12orf65 from a healthy individual. The aligned reads viewed through the Integrative Genomics Viewer (http://www.broadinstitute.org/igv/). A coverage histogram per base is shown above the reads. Amino acid and nucleotide reference sequences are represented on the bottom: green, A; orange, G; red, T; blue, C. B, Scheme demonstrating human C12orf65 gene and protein structure and truncated proteins as a result of previously reported mutations. C, Pedigree of the family from the current study. The proband (whose DNA was a subject to NGS) is indicated with an arrow. Crossed out gray shapes indicate those who have died. The remaining gray shapes are not involved in DNA testing for various reasons. White-colored shapes indicate normal genetic testing. Half black and white shapes represent heterozygous mutation carriers. Pure black shapes represent homozygous mutation carriers. Circles indicate females while squares indicate males.

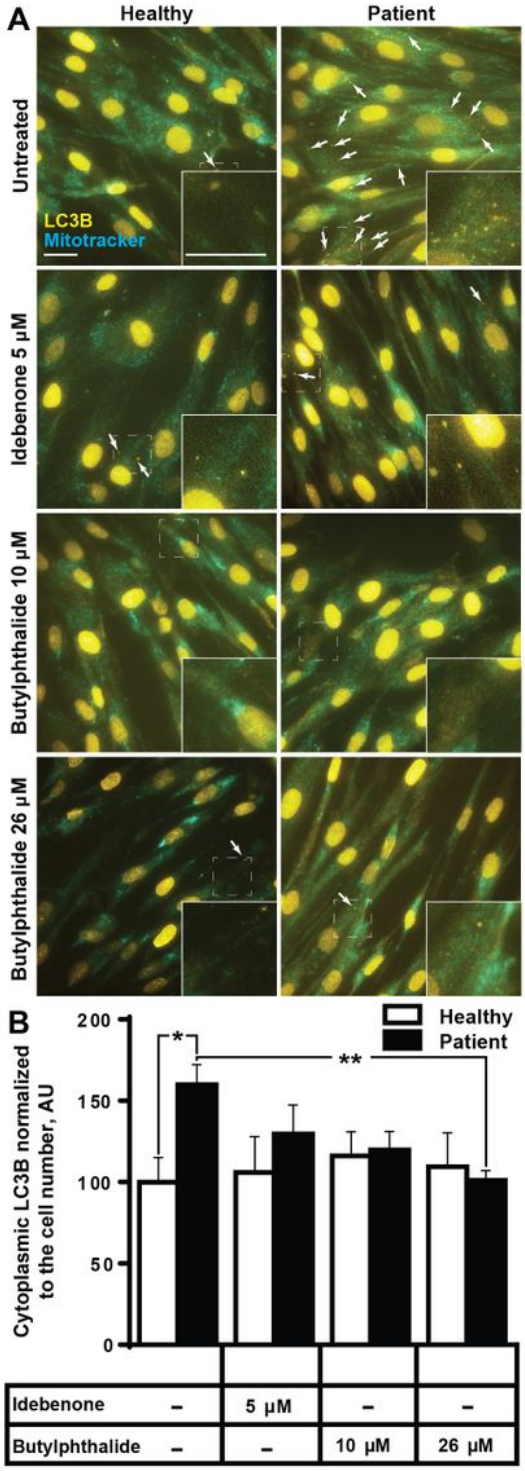

Figure 3

Increased number of LC3B puncta in the primary fibroblasts from the C12orf65-deficient patient. A.B, Representative fluorescent images of primary fibroblasts from a patient and a healthy individual (A) and quantification of the cytoplasmic LC3B immunofluorescence signal with and without treatment with the indicated concentrations of idebenone and DI-3-N-butylphthalide (NBP, butylphthalide) (B). Insets indicate the zoomed out fields with highest number of the LC3B puncta. LC3B signal was normalized to the cell

number in two independent plates with 7-9 wells used for each treatment point and 5 images analyzed per well. The error bars represent S.E.M. *, $P < 0.05$ as determined by ordinary two-way ANOVA followed by Holm-Sidak's multiple comparisons test vs. each healthy individual's fibroblasts in every treatment group. **, $P < 0.01$ as determined by ordinary one-way ANOVA followed by Holm-Sidak's multiple comparisons test at all treated patient groups vs. the untreated patient group. Arrows indicate LC3B puncta. Scale bar, 30 μm.